

# The Surgeon's Third Hand an Interactive Robotic C-Arm Fluoroscope

Norbert Binder<sup>1</sup>, Christoph Bodensteiner<sup>1</sup>, Lars Matthäus<sup>1</sup>,  
Rainer Burgkart<sup>2</sup> and Achim Schweikard<sup>1</sup>

<sup>1</sup>*Institut für Robotik und Kognitive Systeme, Universität zu Lübeck*

<sup>2</sup>*Klinik für Orthopädie und Sportorthopädie, Klinikum Rechts der Isar, TU-München  
Germany*

## 1. Introduction

**Industry** is using robots for years to achieve high working precision at reasonable costs. When performing monotonous work, attention of human operators weakens over time, resulting in mistakes. This increases production costs and reduces productivity. There is also a constant pressure to reduce costs for industrial processes while keeping or increasing their quality.

The idea of integrating robots into the OR was born over a decade ago. Most of these robots are designed for invasive tasks, i.e. they are active tools for medical treatment. Some are telemanipulation systems, filtering tremor and scaling the movements of the user. Others move according to pre-operatively calculated plans positioning instruments of all kinds. Main goal was to achieve a higher precision in comparison to human surgeons, often ignoring the time- and financial aspect. As the economic situation at hospitals becomes more and more strained, economic factors such as costs, time and OR-utilization become more and more important in medical treatment. Now, only few systems can fulfil both requirements: increase precision and reduce the duration of an intervention.



Fig. 1. Robotized C-arm.

We want to introduce another type of robot which assists the surgeon by simplifying the handling of everyday OR equipment. Main goal is to integrate new features such as enhanced positioning modes or guided imaging while keeping the familiar means of operation and improving workflow. The robotic assistance system works in the background until the user wants to use the additional features. On base of a common non-isocentric fluoroscopic C-arm we will explain the way from a manually operated device into an interactive fluoroscope with enhanced positioning and imaging functionality. We first discuss problems of a common C-arm and present possible solutions. We then examine the mechanical structure and derive the direct and inverse kinematics solutions. In the next section, we describe how the device was equipped with motors, encoders and controllers. Finally, we discuss the results of the functionality study and show ways to improve the next generation of robotized C-arms.

## 2. State of the art

### 2.1 Classical Manual C-arm

The common C-arms are small mobile X-ray units. The X-ray source (XR) and the image intensifier (II) are mounted on a C-shaped carriage system. Conventionally there are five serial axes A1 to A5, two of them translational, the rest rotational:

Axis	Parameter	Movement	Name	Function
A1	$d_1$	Trans	Lift	Height adjustment
A2	$\Theta_2$	Rot	Wig-Wag	Rotation in the x-y plane
A3	$d_3$	Trans	Sliding carriage	Arm-length adjustment
A4	$\Theta_4$	Rot	Angulation	C-Rotation sideways
A5	$\Theta_5$	Rot	Orbital Movement	C-Rotation in C-plane

Table. 1. The axes and their names and functions.

The joint arrangement in combination with the C-shape allows for positioning XR and II around a patient who is lying on the OR-couch. Besides of the lift, which is motor-driven, all joints have to be moved by hand one after another: the brake is released, positioning is performed and after reaching the target position, it has to be locked again. As shown in Fig. 2, the axes A4 and A5 do not intersect. In addition, A5 does not intersect the center-beam of the X-ray cone. Therefore, there is no mechanically fixed center of rotation (=isocenter).

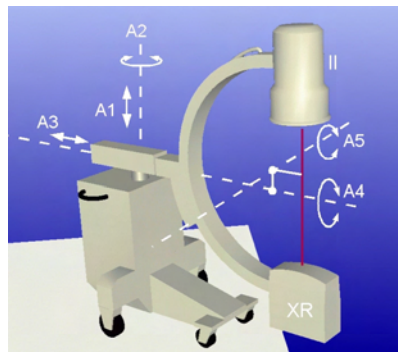


Fig. 2. A common C-arm with the axes A1 to A5.

The overall dimensions and weight of the device are designed for mobility. The C-arm used for our experiments can be moved by one person and fits through normal sized doors. Thus it can be moved from one intervention scene such as OR or ER to the next and is not bound to one room.

## 2.2 Isocentric and semiautomatic C-arms

Meanwhile, industry paid attention to the medical requirements and developed new devices which can deal with the problem of the missing isocenter. The Siemens SIREMOBIL IsoC (Kotsianos et al. 2001, Euler et al. 2002) is constructed with a mechanical isocenter, i.e. A4, A5 and the center-beam intersect in the same point. The radius is fixed, i.e. the distance of the II to the center of rotation cannot be adjusted. As XR and II had to be mounted inside the C to allow for a 190° rotation of joint five, the size of the C had to be increased. Motorization of A5 makes it possible to perform (semi-) automatically data acquisition for 3D reconstruction.

Another system which is the base of this project, is the Ziehm Vario 3D. It has no mechanical isocenter, but when the orbital axis is moved by the user, it can automatically compensate for offsets with the translational joints (Koulechov et al. 2005). This method works for the vertical plane only but it allows for a free selection of the radius within the mechanical limits. The newest version can also perform the orbital movement in a full- or semi-automatically motor driven way. Similar to the Siemens device, data acquisition for 3D reconstruction is realized this way.

## 2.3 Medical problems

When using a standard C-arm fluoroscope two problems occur: First, it is often desired to obtain several images from the same viewing angle during the operation. If the joints were moved after taking the first radiograph, the old position and orientation must be found again. Second, if another image from the same region but from a different angle is required, more than one joint must be adjusted in general. Even basic movements, such as straight-line (translational) movements in the image plane are difficult to perform manually, due to the fact that three of the joints are rotational. Similarly, pure rotations around the region of interest (ROI), if desired, are cumbersome, since two joints are translational, and most of the devices are not isocentric. This shows exemplarily the rather complex kinematics construction of standard C-arms. At the moment handling is done manually and without guidance, which often leads to wrong positioning and thus to a high number of false radiographs, not to forget the radiation dose.

## 3. Computer Simulation

Completing the mechanical work was judged to take some time. Therefore, a software simulation was created to mimic the functionality of the real device. (Gross et al. 2004). It allow for testing and evaluating the primary idea of the project and of a first series of applications (see also section 6).

Additionally, simulated radiographs of our virtual patient can be generated. Image- and landmark-based positioning can be performed the same way as on the real machine now. A comparison of the image quality is given in Fig. 4 for a radiograph of the hip joint. Although the proof of concept study of the mechanical version is completed now, the simulation is still a valuable device for testing new concepts and ideas. Algorithms for collision detection and path planning are now developed on this base.

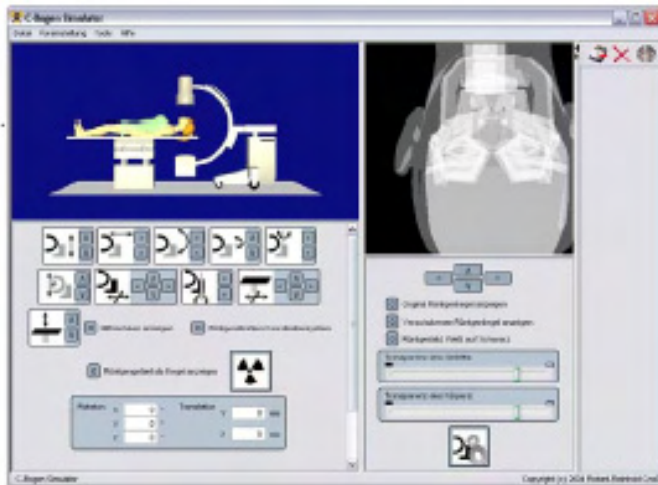


Fig. 3. Screenshot of the simulation GUI.

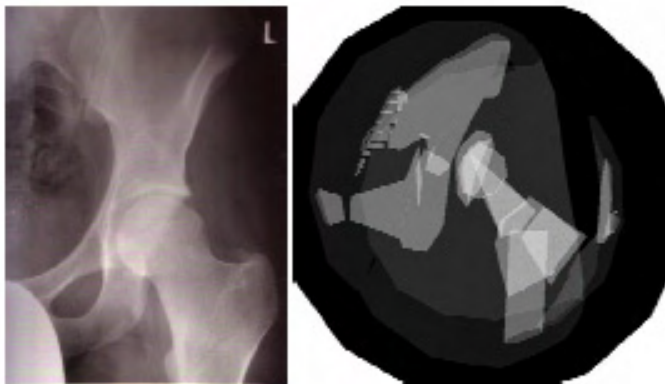


Fig. 4. Comparison of real radiograph and simulation for a hip joint.

## 4. Realisation

The C-arm has five serially arranged joints, which limit the ability for free positioning in 3D space to 5 DOF. Image-plane and -center can be selected freely but the rotation around the beam axis depends on the first parameters.

The challenges of the hardware part of robotization lie in the movement of big masses with high precision and OR acceptable speed. Thus, careful selection and integration of motors, controllers and encoders is important for the success and are therefore subject of discussion in this study.

### 4.1 Proof of concept study

Basis of our work was a C-arm with motorized lift (joint one) and arm-stretch (joint three). Position encoders were included for these joints, too, but also for the orbital movement (joint

five). Communication to an integrated PC via SSI allowed for isocentric movements in the vertical plane (Koulechov et al. 2005).

For our project, a fully robotized device was required (Binder et al, 2005). In a first step, we measured the forces and torques during acceleration and motion. On this information, drives, gears, and encoders were selected. Due to lack of space inside the device, external mounting was favoured. This also guarantees a high flexibility in changing and adapting single components for improvement throughout the development process.

Communication to the control PC was established via a fieldbus system and a programmable control-unit on a PCI-card. The existing communication had to be replaced as it could not fulfill the requirements of our system and did not offer the same comfortable interface for programming.



Fig. 5. Joints two, four and five with external drives, gears and encoders.

After implementation of some test routines, the applications were transferred from simulation onto the real system. The tests were successful and indicated the high potential of the motorized system (Binder et al. 2006). Some of the results are shown in the application-section. Knowing about the precision required for positioning for some of our applications like 3D reconstruction, we developed a setup that allowed for registering the real C-arm to the kinematical model. Positions and orientations were measured by an infrared tracking system and then compared to those we calculated.

#### 4.2 Experiences

Positioning the C-arm with our software can be done easily and shows that the idea will work out. Therefore it is sure that a minimum of costs and effort can help to improve the workflow in mobile X-ray imaging.

Nevertheless, there are still some problems to overcome. The weights which have to be moved here require a high gear reduction. Moving the joints manually is therefore hard to manage as it requires a lot of strength, that would damage the gears. We will integrate a different coupler in the next generation. Meanwhile the semi-manual handling, i.e. motor-assisted movements, which were in the first place integrated for weight compensation, performs very promising and will be part in the next generation, too. Additionally, effects of mechanical deformation and torsion during positioning are too big, too, and cannot be ignored. Right now we are working on several methods to compensate for these errors. The results will be published later. High masses in combination with friction also influence the positioning accuracy. Especially joints two and four are subject of further improvement. For better motor-controlling and to minimize effects of torsion and elasticity in the drive-axis and belts, the position encoders will be positioned at the driven part as originally planned.

The next generation of our C-arm will integrate the experiences we have obtained and allow for further evaluation.

## 5. Kinematics

Now that the C-arm joints can be moved motor driven, some of the applications such as weight compensation can already be realized. But performing exact positioning requires knowledge about the relationship between joint parameters and C-arm position and orientation. This so-called kinematic problem consists of two parts. The direct kinematics, i.e. calculating position of the ROI and orientation of the beam from given joint parameters can be derived by setting up the DH-matrices and multiplying those one after another. These basics are described e.g. in (Siegert, HJ. & Bocioneck S. 1996). For most applications ROI and beam direction are given from the medical application and with respect to the C-arm base or a previously taken radiograph. The joint-parameters for this new position have to be calculated. This is the so-called inverse kinematic problem. In the following section we want to introduce a geometry based solution.

### 5.1 Inverse kinematics

Conventional C-arms have five joints and thus are limited to 5 DOFs. The consequence is that the rotation of the radiograph around the center beam depends on the position  $\bar{p}$  of  $O_z$  (=ROI) and the beam direction  $\bar{m}_z$  which defines the z-axis of our tool coordinate system. From the transformation matrix  ${}^0M_5$  we therefore know only those two vectors:

$${}^0M_5 = \begin{pmatrix} ? & ? & m_{zx} & p_x \\ ? & ? & m_{zy} & p_y \\ ? & ? & m_{zz} & p_z \\ 0 & 0 & 0 & 1 \end{pmatrix} \quad (1)$$

Table 2: Information given for the inverse kinematics. introduces the basic variables in this calculation. They are illustrated in Fig. 2 and Fig. 7. Axes Fig. 7 Axes and vectors used for inverse kinematics.

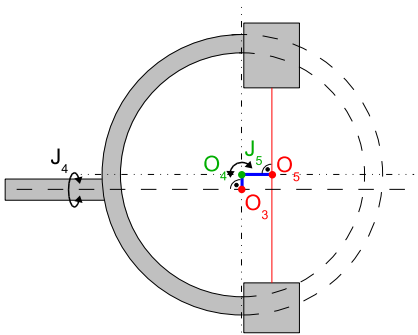


Fig. 6. mechanical offsets of the system.  $O_4$  is the rotational center of the C and  $O_5$  the center between image intensifier and generator.

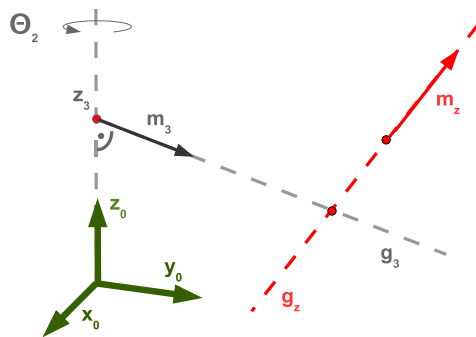


Fig. 7. Axes and vectors used for inverse kinematics.

$K_0$	Base coordinate system with $x_0, y_0, z_0$
$z_0$	Translational axis of joint 1 rotational axis of joint 3
$O_5$	Midpoint between XR and II.
$O_z$	Target (= ROI), $O_5 = O_z$ in case the default radius is used. $O_z$ can be moved along the center beam to adapt the radius $XR \leftrightarrow ROI$ .
$\vec{m}_z$	Beam Direction
$\vec{g}_z = O_z + s \cdot \vec{m}_z$	Center beam of x-ray cone with direction $\vec{m}_z$ through ROI $O_z$
$\vec{m}_3$	Direction of arm, parallel to $x_0, y_0$ -plane Rotational axis for joint 4
$\vec{g}_3 = \vec{h}_3 + t \cdot \vec{m}_3$	Line along arm at height $d_1$ with direction $\vec{m}_3$ , intersecting $\vec{g}_z$

Table 2. Information given for the inverse kinematics.

The idea of this calculation is now to reduce the number of unknown joint parameters by applying geometrical knowledge and interdependencies.

As illustrated in Fig. 7., the translational axis  $\vec{g}_3$  with direction vector  $\vec{m}_3$  describing the arm, depends directly on  $\theta_2$ . Equating  $\vec{g}_3$  and  $\vec{g}_z$  allows for expressing the height of the arm  $d_1$  as a function of  $\theta_2$ :

$$\vec{g}_3 = O_2 + t \cdot \vec{m}_3 \tag{2}$$

$$= \begin{pmatrix} 0 \\ 0 \\ d_1 \end{pmatrix} + t \cdot \begin{pmatrix} -\sin(\Theta_2) \\ \cos(\Theta_2) \\ 0 \end{pmatrix}$$

$$\vec{g}_z = O_z + s \cdot \vec{m}_z \tag{3}$$

$$= \begin{pmatrix} O_{zx} \\ O_{zy} \\ O_{zz} \end{pmatrix} + s \cdot \begin{pmatrix} m_{zx} \\ m_{zy} \\ m_{zz} \end{pmatrix}$$

$$d_1 = O_{zz} - m_{zz} \frac{O_{zx} - O_{zy} \tan(\Theta_2)}{m_{zx} + m_{zy} \tan(\Theta_2)} \tag{4}$$

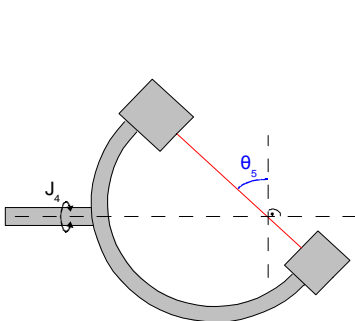


Fig. 8.  $\theta_5$  is derived in the C-plane on base of  $\vec{g}_3$  and  $\vec{g}_z$ .

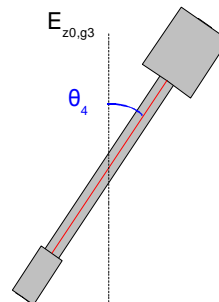


Fig. 9.  $\theta_4$  in the mechanical system, looking along  $\vec{g}_3$  towards the C-arm base.

These functions can now be used to calculate the joint parameters for A4 and A5. Two planes have to be defined for further work: The C-plane  $E_C$  with normal vector  $n_C$  and the  $z_0g_3$ -plane with normal-vector  $\bar{n}_{03}$  :

$$n_C = \bar{g}_3 \times \bar{g}_z \quad (5)$$

$$n_{03} = \bar{g}_3 \times \bar{z}_0 \quad (6)$$

$|\Theta_4|$  is the angle between the C-plane and the  $z_0g_3$ -plane (see Fig. 9). Its sign is decided in dependency of  $\bar{n}_{03}$  and the part  $\bar{g}_{z||n}$  of  $\bar{g}_z$ , which is parallel to  $\bar{n}_{03}$  :

$$\text{sign}(\Theta_4) = \begin{cases} 1 \text{ for } \bar{g}_{z||n} \parallel \bar{n}_{03} \\ -1 \text{ for } \bar{g}_{z||n} \Downarrow \bar{n}_{03} \end{cases} \quad (7)$$

$|\Theta_5|$  is given by the angle between  $\bar{g}_z$  and  $\bar{g}_3$ . To fit into our definitions, this value is subtracted from  $\frac{\pi}{2}$  (see Fig. 8). The sign is fixed by extracting the part  $\bar{g}_{z||3}$  from  $\bar{g}_z$ , which is parallel to  $\bar{g}_3$  :

$$\text{sign}(\Theta_5) = \begin{cases} 1 \text{ for } \bar{g}_{z||3} \parallel \bar{g}_3 \\ -1 \text{ for } \bar{g}_{z||3} \Downarrow \bar{g}_3 \end{cases} \quad (8)$$

The last missing joint parameter is the length of the arm, i.e. the horizontal distance between  $O_2$  and  $O_3$  (see Fig. 10). Due to the mechanics, the following information is given:

$[O_5, O_4]$	Perpendicular to $\bar{g}_z$ , length $a_5$ , in $E_C$ ,
$[O_4, O_3]$	Perpendicular to $\bar{g}_3$ , length $a_4$ , in $E_C$ ,

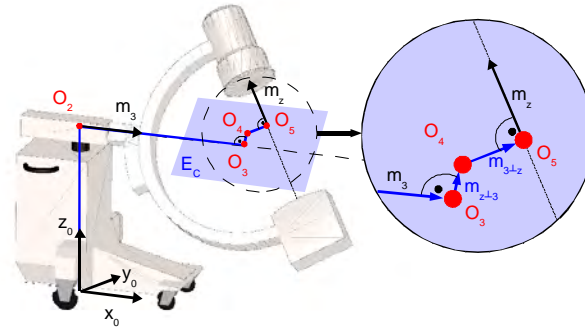


Fig. 10. Projection into the  $E_C$  plane.

To get the correct directions vectors, the vectors are defined:

$\bar{m}_{3\perp z}$	Part of $\bar{m}_3$ perpendicular to $\bar{m}_z$
$\bar{m}_{z\perp 3}$	Part of $\bar{m}_z$ perpendicular to $\bar{m}_3$

Now starting at  $O_5$ ,  $O_4$  and  $O_3$  can be calculated:

$$O_4 = O_5 - a_5 \cdot \bar{m}_{3\perp z} \quad (9)$$

$$O_3 = O_4 - a_4 \cdot \bar{m}_{z\perp 3} \quad (10)$$

The armlength is then:

$$d_3 = \sqrt{O_{3x}^2 + O_{3y}^2} \quad (11)$$

As defined at beginning of this section, 3  $gv$ ,  $z$   $gv$ , and all their parts are functions of 2. Therefore the calculated functions for the joint parameters  $d_1$ ,  $d_3$ , 4  $\Theta$ , and 5  $\Theta$  depend on 2, too. When inserting them into the homogeneous transformation matrix  ${}^0_{A_5}(d_1, \Theta_2, d_3, \Theta_4, \Theta_5)$ , we get by symbolic calculation of the direct kinematics, we get  ${}^0_{A_5}(\Theta_2)$ .

The correct  $\Theta_2$  is found by determining the zero of the difference function between the position  $\bar{p}(\Theta_2)$  and orientation  $\bar{z}(\Theta_2)$  from  ${}^0_{A_5}(\Theta_2)$  and the given target parameters  $\bar{p}$  and  $\bar{z}$ . This can be done by numerical means.

There is one case which has to be dealt with separately. For  $\Theta_5 = -90^\circ$ ,  $\bar{m}_z$  is anti-parallel to  $\bar{m}_3$ . The lines have the distance  $d_{45} = a_4 + a_5$  and are parallel to the  $x_0y_0$ -plane, i.e.  $m_{zz} = 0$ . As they do not intersect, the approach introduced above cannot be used. When starting the inverse kinematics an intersection cannot be determined and  $\Theta_5$  is still unknown. Checking for  $m_{zz} = 0$  is a necessary constraint but also includes all  $\Theta_5$  for  $\Theta_4 = \pm\pi$ . This can be filtered out by checking the distance  $d$  between  $z_0$  and  $\bar{g}_z$ . As illustrated in Fig. 11, the maximum is given by  $d_{45}$ . For  $d > d_{45}$  the calculation can be done as mentioned above, otherwise, the following solution has to be used.

Projection into the  $x_0y_0$ -plane simplifies the calculation.  $d$  is the distance between  $\bar{m}_z$  and  $\bar{m}_3$  when projected into this plane.  $\Theta_4$  can now be derived using  $d$  and  $d_{45}$ . The sign of  $\Theta_4$  is determined by the intersection  $i$  of  $\bar{m}_z$  with the  $x_0$ -axis.

$$\Theta_4 = \arcsin\left(\frac{d}{d_{45}}\right) \quad (12)$$

$$\text{sign}(\Theta_4) = \begin{cases} +1 & \text{for } i \leq 0 \\ -1 & \text{for } i > 0 \end{cases} \quad (13)$$

$d_3$  is calculated from  $d$  and  $l$  using the theorem of Pythagoras. Now the value of  $\Theta_2$  can be derived.

$$|\alpha| = \left| a \sin\left(\frac{d}{l}\right) \right| \quad (14)$$

$$\delta = a \tan\left(\frac{p_x}{p_y}\right) \quad (15)$$

$$\Theta_2 = \delta - \text{sign}(\Theta_4) \quad (16)$$

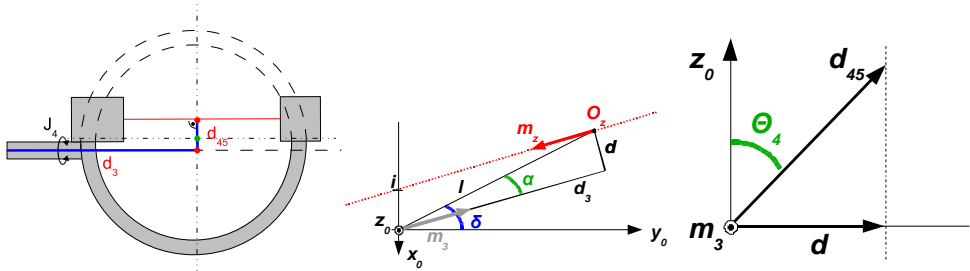


Fig. 11. Special case:  $\Theta_5 = -90^\circ$ .

## 6. Applications

When this project started, the major goal was to simplify the handling of the C-arm. The user should be able to reach the intended target position in terms of a point and shoot procedure known from photo cameras. Thinking about which joint has to be moved in which way to reach the right position should no longer be necessary. Positioning has to be performed by means of the radiographs taken and in terms of left/right, up/down, forward/backward. This way we wanted to get away from the trial and error solution. Nevertheless, the common way of handling the C-arm has to be kept. Several reasons have to be mentioned for that; Safety in critical situations, “backward-compatibility” for people who want to get used to the system step by step and finally for those users, which don’t want to use a robotic system for whatever reason.

In the following sections, we give a number of examples that can already be performed on the current version of our robotized C-arm. We achieved not only simplified positioning, but also opened a way for completely new applications. Due to the close cooperation with surgeons, more will follow, soon.

These examples also make clear, that the staff in the operation theatre will be in full control of the device at every time. None of these applications has to be performed in an assisted way, as the common means of handling are still available and override all other actions. However, if the user wants to use one of the additional functions offered, they are available.

### 6.1 User Controlled Movements

#### 6.1.1 Semi-manual positioning

The moving parts of the C-arm are weight-balanced and thus can be moved easily. Nevertheless, in some positions the manual acceleration of image-intensifier and generator requires some strength. Applying the drives, gears, and couplers for the robotized system increases friction. To ease the effort, the user-intention for the movements of each single joint is recognized and the drives move accordingly. Thus, a simple weight compensation is realized.

As already mentioned above, purely manual positioning is not possible at the moment, but will be available after some changes in the mechanical system in the next generation. Even in the worst case scenario of a power failure, the C-arm can be moved away from the patient to ensure a safe surgery.

#### 6.1.2 Cartesian Movements

When operating the standard mechanical C-arm by hand, joint parameters were changed one after the other. The non-trivial architecture of the fluoroscope leads to complex changes

of the region of interest and the viewing direction when moving a joint. Thus it is difficult to set the parameters of the C-arm for a certain region of interest. Using the inverse kinematics, movements along Cartesian axes can be performed easily. Those motions are much easier to visualize by humans and allow for faster positioning. Here it makes no difference which coordinate system is used. The translations and rotations can be specified in relation to the C-arm, to the patient, or to the radiograph. The latter allows for shifts in the image plane, in order to recenter (coordinates  $x$  and  $y$ ) or to obtain a closer view (coordinate  $z$ ). The new target position can be marked directly on the radiograph, e.g. on a touch-screen. To make positioning even easier, a simulation of the new image - based on previous pictures - can be presented to the OR staff on the computer screen.

### 6.1.3 Isocentric Rotation

As already noted, common C-arm designs were not optimized for isocentric movements due to manufacturing reasons, i. e. when moving joints four and/or five, the image center will change. This complicates image acquisition of a ROI from different viewing angles.

Unlike other systems (Koulechov K., 2005, Moret, J, 1998), we are not limited to one fixed plane or a fixed distance to the center of rotation but can reach all possible positions in between the mechanical limitations. Using the inverse kinematics, we can easily rotate the C-arm with a user specified distance around an arbitrary point and in an arbitrary plane. All the surgeon has to do is to define the center of the rotation, either by marking a point in an image - an fast, but somewhat inaccurate way - or by marking the same landmark in two different images to allow for the extraction of 3D-coordinates of the desired fixed point - the exact way. The plane of the rotation can be defined by the plane of the C of the fluoroscope or by defining any two linearly independent vectors centered on a fixed point.

## 6.2 Automatic Positioning

### 6.2.1 Re-centering

Placing the C-arm in such a way that a given ROI will be imaged is often difficult and requires experience, especially when the patient is corpulent. If for example an image of the femur head has to be obtained, its center should be in the center of the radiograph. If an image is not centered properly and the ROI is on the edge of the radiograph, important information might be cut off.

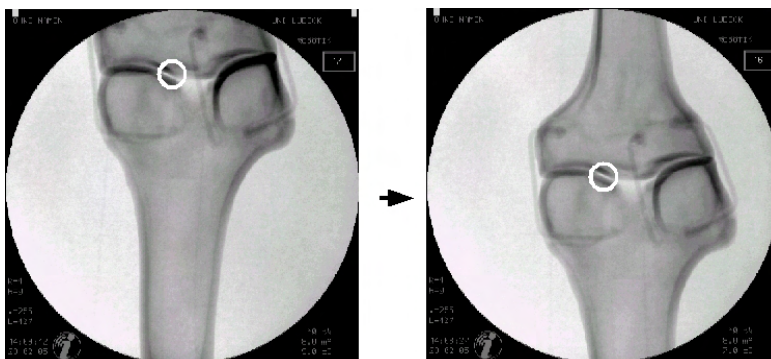


Fig. 12. Selecting the new center on a misplaced radiograph for automatic repositioning.

Nevertheless, the picture can still be used to obtain a corrected image. After marking the desired center in the old image, the robotic C-arm can automatically reposition itself such that the desired region is mapped at the center. The viewing angle can either be corrected before taking the new image or be kept from the old image.

### 6.2.2 Standard Images

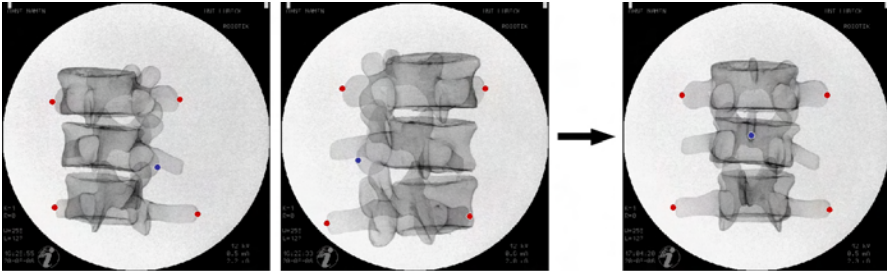


Fig. 13. Defining landmarks on two radiographs for exact automatic a.-p. positioning on a vertebra.

Many radiographs are views of standard planes e. g. anterior-posterior, lateral, medial etc. A motorized C-arm can be moved easily to these positions. In order to enable the robotic C-arm to move to the desired position, the surgeon identifies several landmarks on two pictures of the ROI taken from different angles. The 3D-coordinates of the landmarks are calculated internally and the correct image center and image direction are calculated based on the inverse kinematics. The latter one relies on marking special landmarks from which to get the right anatomical position for the image. E. g. for a-p-images of the spine the surgeon would mark the left and right transverse process and the spine of the vertebra to define the region of interest as well as the a-p-direction (see Fig. 13). It should be mentioned that other image modalities can be easily included into the set of standard images by defining the number of points to be marked and the algorithm describing the ROI and beam direction in terms of the marked points.

### 6.3 Image Sequences

One of the most interesting perspectives for a motorized C-arm are applications which need the input of more than one image. These applications require an exact calibration of the generated image (Brack et al. 1996 & 1999)\* and compensation of the mechanical deformations caused by the masses of the source and the detector. Due to the integrated position encoders for each joint, position and orientation of each image is known. Therefore, we also know the relationship between all images taken (as long as the C-arm base is not moved).

#### 6.3.1 Longbone And Poster Images

Some structures in the human body are bigger than the field of view of the fluoroscope. In orthopaedics, sometimes images of the whole femur are useful. Neurosurgeons may have to scan the whole spine to find the vertebra of interest. Images of the entire thorax or pelvis are important in emergency rooms or surgery. Currently the field of view of the standard C-arm is very limited (a 17 cm diameter circular image is typical). Our solution is to acquire several

images and compose a single image by (semi-)automatic positioning of the C-arm during image collection. By marking the starting point on two images from different angles its position in space can be calculated. After defining a target point in the same way, the angle of view (a-p, lateral or user-defined) is set. Depending on the distance between start- and end-point, the C-arm will take a series of radiographs and will align them to one single longbone-image. Our longbone-application offers user-interactive image acquisition.

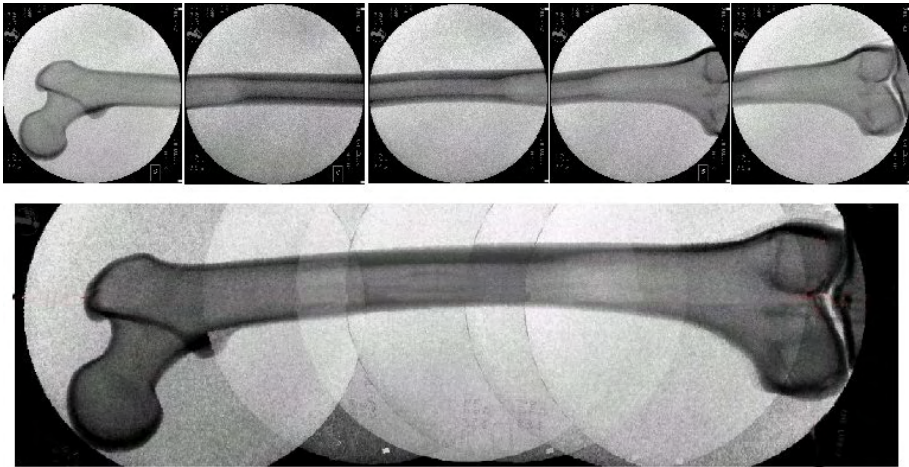


Fig. 14. Radiographs and combined longbone-panorama from real experiments with the C-arm.

It is a non-trivial task to align single images for manual long-bone-image construction. Different methods, such as X-ray rulers (Yaniv Z. & Joskowicz L., 2004) were suggested for registration. In our approach, position and orientation of the images in space are given by the position encoders and are saved with the image data. Therefore, it is not difficult to combine the images with a minimum effort of registration. The result shown in Fig. 14 was reconstructed with the given joint parameters only, i.e. no additional registration was applied.

For emergency radiographs, marking start- and endpoint in two images each will take too long. Thus, only the start point and a direction-vector are marked in the first image and the fluoroscope moves in the indicated direction parallel to the image plane taking a specified number of radiographs. Additionally, the direction of movement might be corrected during processing.

An application similar to the longbone sequence is taking an image of the whole thorax. There, not only one row of images but a whole matrix of images must be taken and combined in the correct way. It is easy to see that our approach extends to this application naturally. It has to be mentioned that due to the form of the x-ray cone, deep objects will achieve projection errors when overlapping the single radiographs. This is a problem which all cone-beam machines have to overcome. For single bones such as the femur shown in Fig. 14, these errors are less than 1 mm.

### **6.3.2 Intra-surgical data collection for 3D reconstruction**

In some surgeries, 3D-images of bones or other body structures substantially help to get better orientation and control. Acquiring such image data in a standard OR is complicated

as a CT is normally not available. With the help of the fluoroscope robot, CT-like 3D-images can now be acquired. For this, the C-arm is rotated around the ROI in small discrete steps in an isocentric movement. In each step, a radiograph is taken. The rotation plane can be selected freely within the mechanical limits of the C-arm.

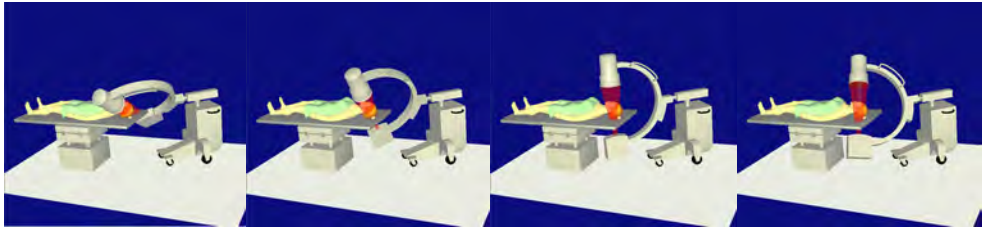


Fig. 15. Collecting radiographs for 3D reconstruction.

A 3D model of the ROI can be calculated with an iterative reconstruction algorithm, e.g. the algebraic reconstruction technique (ART) algorithm (Toft P. 1996), in reasonable time. The achieved 3D resolution is sufficient for many diagnostic means and rises with the increasing resolution of the image intensifier. Unlike (Ritter et al. 2003), about 20-50 images are necessary to create a sufficient 3D image of the target. Furthermore, the distance between the ROI and the detector-screen can be varied freely and is not fixed.

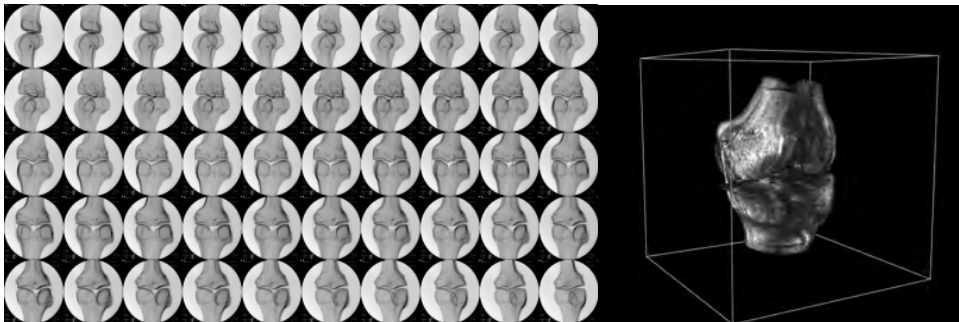


Fig. 16. Series of projections and the reconstructed result.

## 7. Results and Future Work

Experiments with this world's first fully robotized C-arm show very promising results. Movements in the image plane, longbone images, data acquisition for 3D reconstruction, and landmark based positioning were successfully implemented and tested. The next version of our C-arm will overcome mechanical problems such as lacking positioning accuracy and mechanical deformation.

The value of an every-day OR-device can be increased by simple means. The workflow can be optimized and mistakes can be prevented. Operation time is saved and radiation dose for patient and staff is minimized. The experiences of this study have already been transferred to other systems such as OR microscope (Knopp et al. 2004) and showed similar promising results. Chances are that the number of such robot- assisted systems in the OR will increase soon.

## 8. References

- Binder, N., Matthäus, L., Burgkart, R. & Schweikard A., A Robotic C-arm Fluoroscope Int. Journal on Medical Robotics and Computer Assisted Surgery, Vol. 1, Issue 3, ISSN 1478-5951, 108-116, John Wiley & Sons, Ltd. (www.roboticpublications.com), Ilkley, UK, 2005
- Binder, N., Bodensteiner, C., Matthäus, L., Burgkart R. & Schweikard A., Image Guided Positioning For an Interactive C-arm Fluoroscope, Proc. Computer Assisted Radiology and Surgery (CARS), Osaka, Japan, 2006
- Brack C. , Götte H., Gosse F., Moctezuma J. et al., "Towards Accurate X-Ray-Camera Calibration in Computer-Assisted Robotic Surgery," Proc. Int. Symp. Computer Assisted Radiology (CAR), pp. 721-728, 1996, paris.
- Brack C., Burgkart R., Czopf A., et al. "Radiological Navigation in Orthopaedic Surgery," Rechnergestützte Verfahren in Orthopädie und Traumatologie, p 452ff, 1999, steinkopf-Verlag.
- Euler, E., Heining S., Fischer T., Pfeifer K. J. & W. Mutschler, Initial Clinical Experiences with the SIREMOBIL Iso-C3D, electromedica 70 (2002) no. 1
- Groß R., Binder N. & Schweikard A., "Röntgen-C-Bogen Simulator," Proc. Computer und Roboterassistierte Chirurgie, Abstract CD-ROM, 23, Deutsche Gesellschaft für Computer- und Roboterassistierte Chirurgie , auch: www.medicstream.de, München, 2004
- Kotsianos, D., Rock, C., Euler, E., Wirth, S., Linsenmaier, U., Brandl, R., Mutschler, W. & Pfeifer, K. J., 3D-Bildgebung an einem mobilen chirurgischen Bildverstärker (ISO-C-3D) Erste Bildbeispiele zur Frakturdiagnostik an peripheren Gelenken im Vergleich mit Spiral-CT und konventioneller Radiographie, Der Unfallchirurg, Band 104, No. 9, 2001, Springer Berlin / Heidelberg, ISSN: 0177-5537 (Paper) 1433-044X (Online)
- Knopp, U., Giese, A., Binder, N. & Schweikard, A., Roboterunterstützung eines OP-Mikroskops, Proc. Computer und Roboterassistierte Chirurgie 2004, Abstract CD-ROM, 23, Deutsche Gesellschaft für Computer- und Roboterassistierte Chirurgie , auch: www.medicstream.de, München, 2004
- Kotsianos, D, Rock, C, Euler, E et. al., 3D-Bildgebung an einem mobilen chirurgischen Bildverstärker (Iso-C 3D): Erste Bildbeispiele zur Frakturdiagnostik an peripheren Gelenken im Vergleich mit Spiral-CT und CT konventioneller Radiologie. Unfallchirurg 2001; 104(9): 834ff
- Koulechov K., Lüth T., Tita R. "Freie Isozentrik und 3D-Rekonstruktion mit einem Standard C-Bogen", atp Automatisierungstechnische Praxis, 05/2005
- Moret, J, 3D-Rotational Angiography: Clinical value in endovascular treatment, Philips medical, [http://www.medical.philips.com/us/products/cardiovascular/assets/docs/Application\\_note\\_Moret.pdf](http://www.medical.philips.com/us/products/cardiovascular/assets/docs/Application_note_Moret.pdf), Medical Mundi, 1998
- Ritter, D. Mitschenke, M. & Graumann, R., Intraoperative soft tissue 3D reconstruction with a mobile C-arm. International Congress Series, 2003, 1256:200-6, doi:10.1016/S0531-5131(03)00243-7
- Siegert, HJ. and Bocionek, S., Robotik: Programmierung intelligenter Roboter. Springer-Verlag, 1996.

- Toft, P., "The Radon transform - Theory and Implementation," Ph.D. Thesis, Department of Mathematical Modelling, Section for Digital Signal Processing, Technical University of Denmark, 1996.
- Yaniv, Z. and Joskowicz, L., "Long bone panoramas from fluoroscopic x-ray images," IEEE Transactions on Medical Imaging, vol. 23, pp. 26-35, 2004.